Magnetic field generation via Kelvin-Helmholtz instability in sheared astrophysical plasmas, using relativistic particle-in-cell (R-PIC) simulations

Ioana Duţan
Institute of Space Science (ISS), Bucharest, Romania

work with Ken-Ichi Nishikawa (NSSTC/Alabama Univ.), Huntsville, USA

23 January 2013

OVERVIEW

- Introduction
- Simulation of kinetic Kelvin-Helmholz instability (KHI)
- Initial conditions and numerical results
- Summary and conclusions

OVERVIEW

- Introduction
- Simulation of kinetic Kelvin-Helmholz instability (KHI)
- Initial conditions and numerical results
- Summary and conclusions

OVERVIEW

- Introduction
- Simulation of kinetic Kelvin-Helmholz instability (KHI)
- Initial conditions and numerical results
- Summary and conclusions

OVERVIEW

- Introduction
- Simulation of kinetic Kelvin-Helmholz instability (KHI)
- Initial conditions and numerical results
- Summary and conclusions

Introduction

Active Galactic Nuclei (AGN) spectra

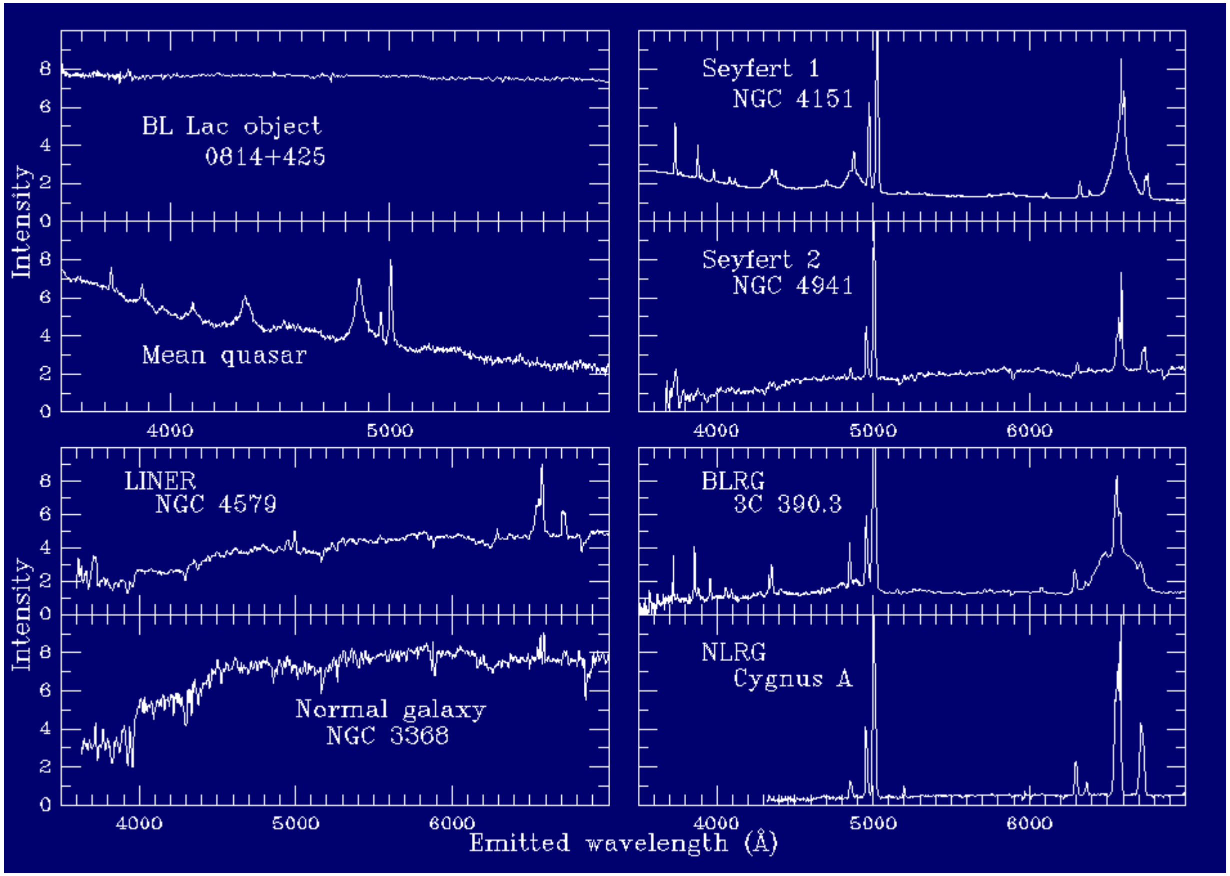

- AGN = galaxies whose nucleus spectrum cannot be explained by standard stellar physics, e.g., a dense stellar cluster of massive stars or a stellar mass BH

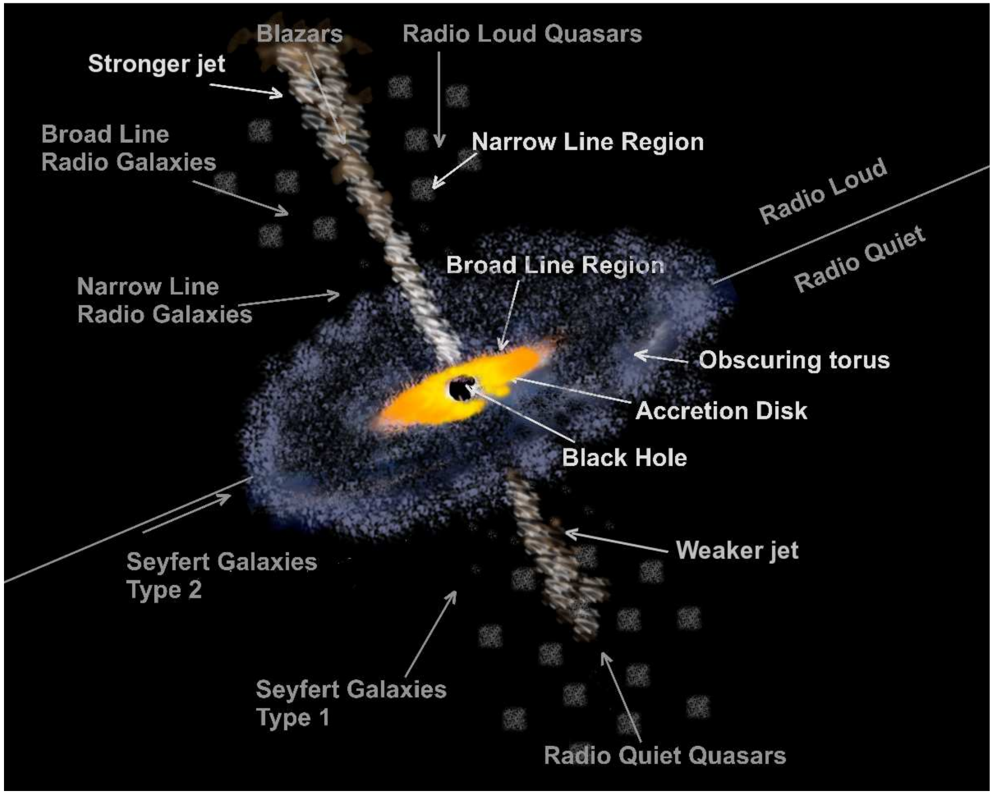

- spinning supermassive BH, $M \sim 10^7 - 10^9 M_\odot$, surrounded by an accretion disk

- AGN jets: $v_{\rm jets} \sim 0.9 - 0.995c$ or $\gamma = 2 - 10$ (bulk Lorentz factor)

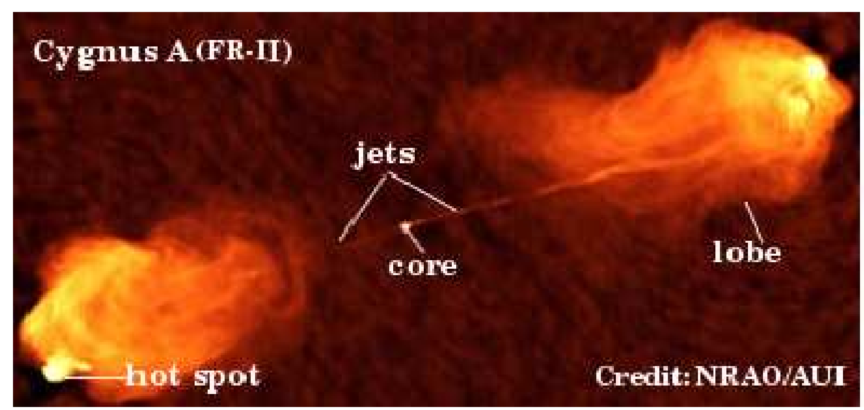

Spectrum

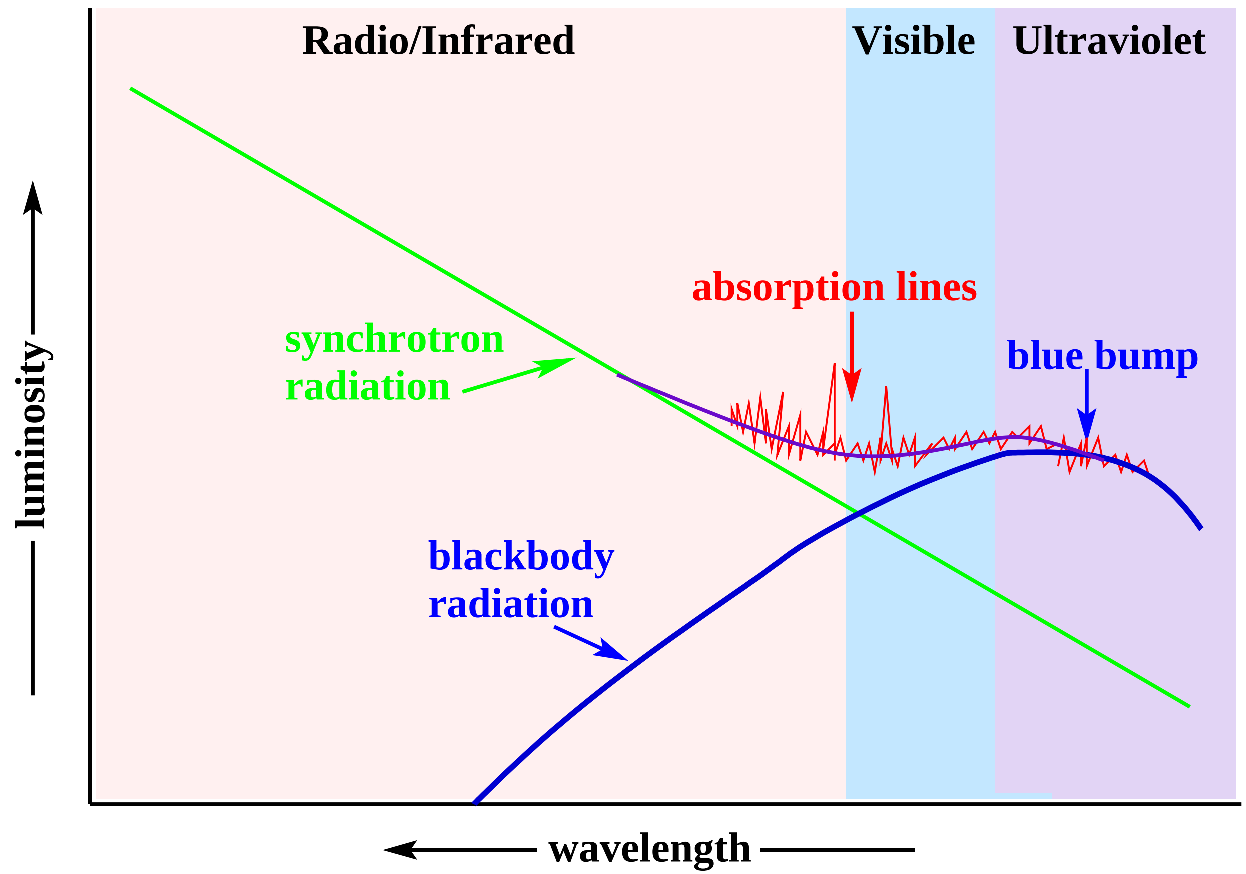

- power-law (non-thermal) radiation ($\nu^{-\alpha}$): jets
- blackbody (thermal) radiation: accretion disk

Spectrum

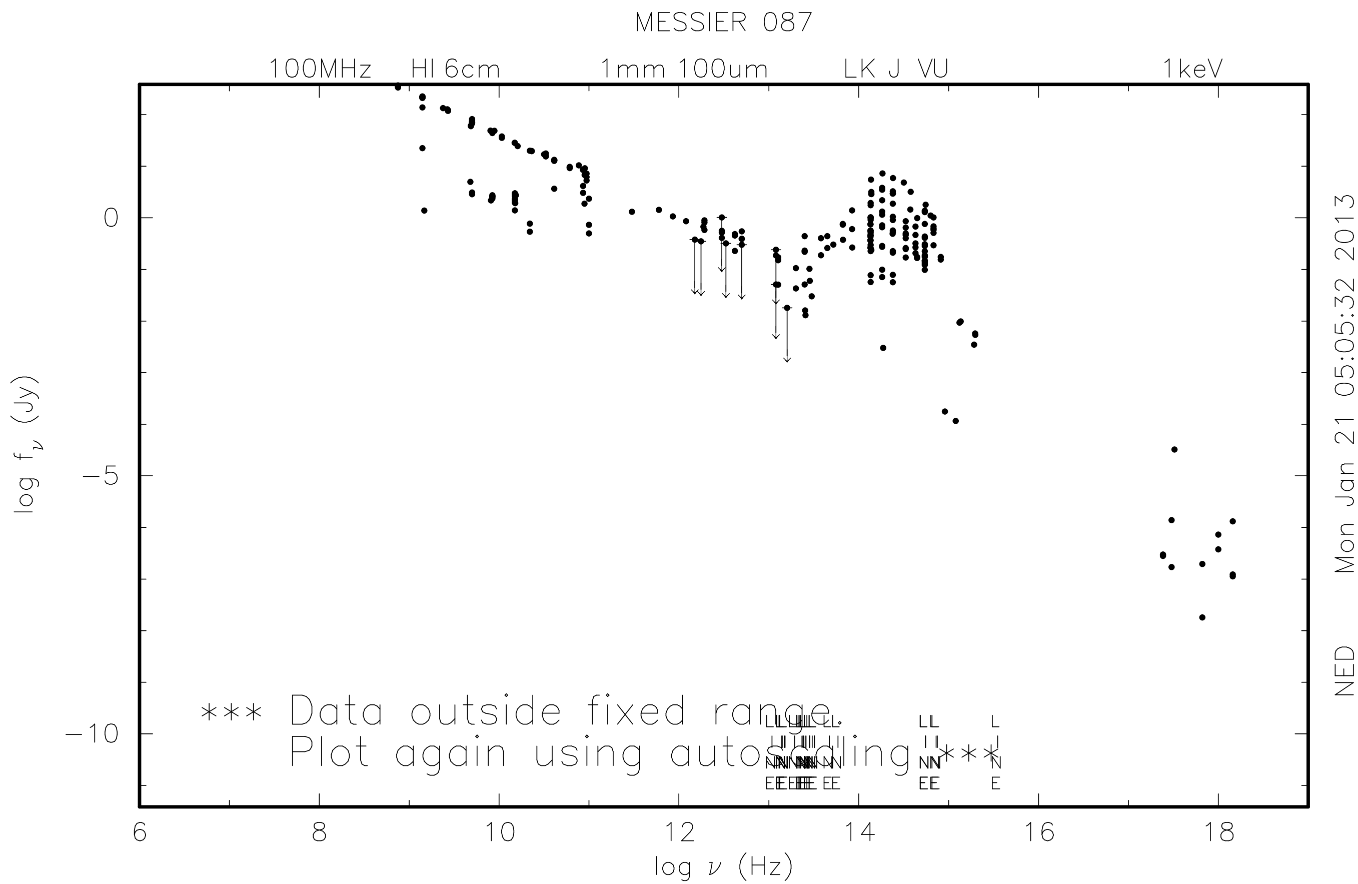

- M87 spectral energy distribution

Synchrotron radiation from AGN jets: M87

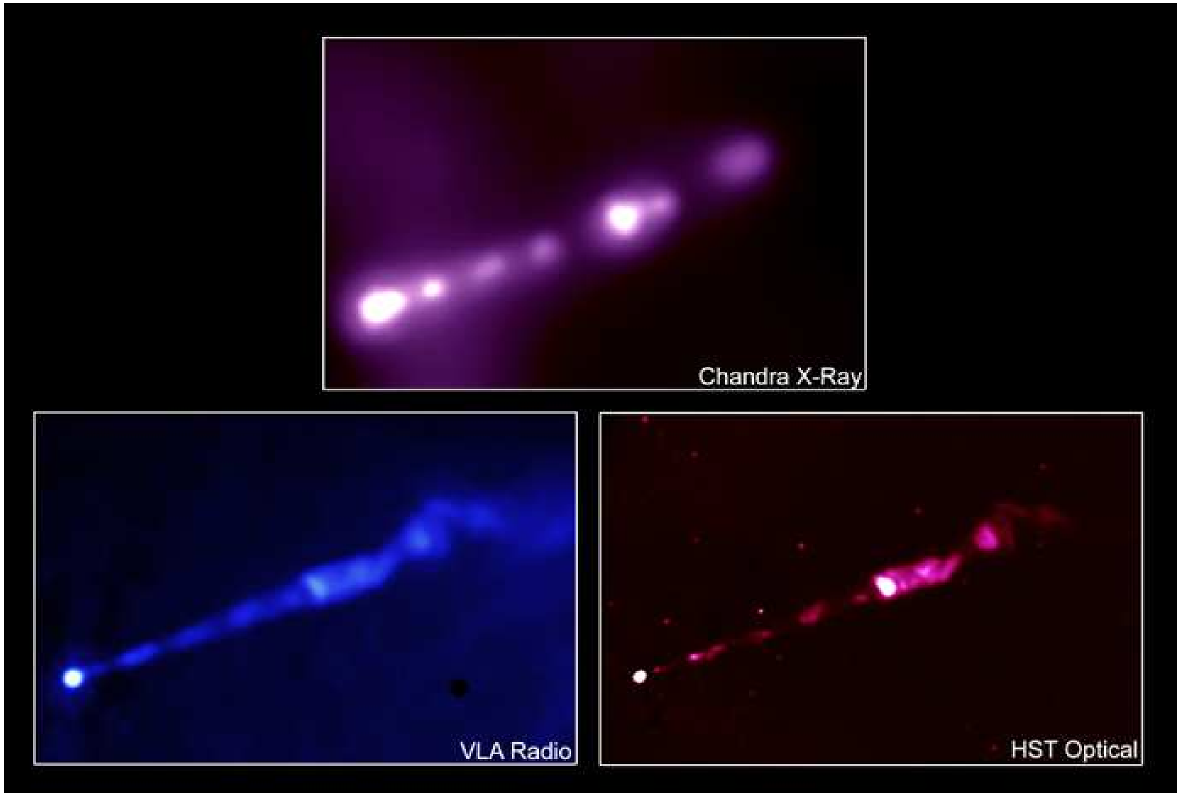

- synchrotron emission over the whole continuum spectrum

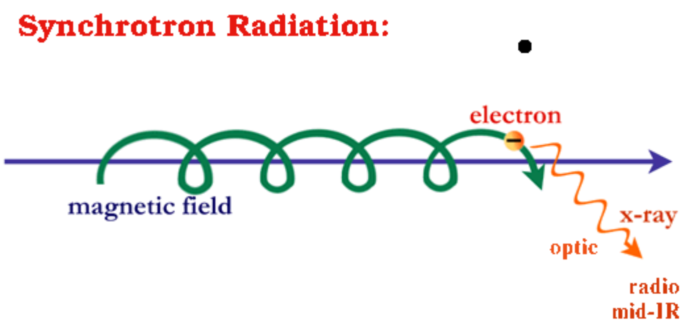

Synchrotron radiation from AGN jets: M87

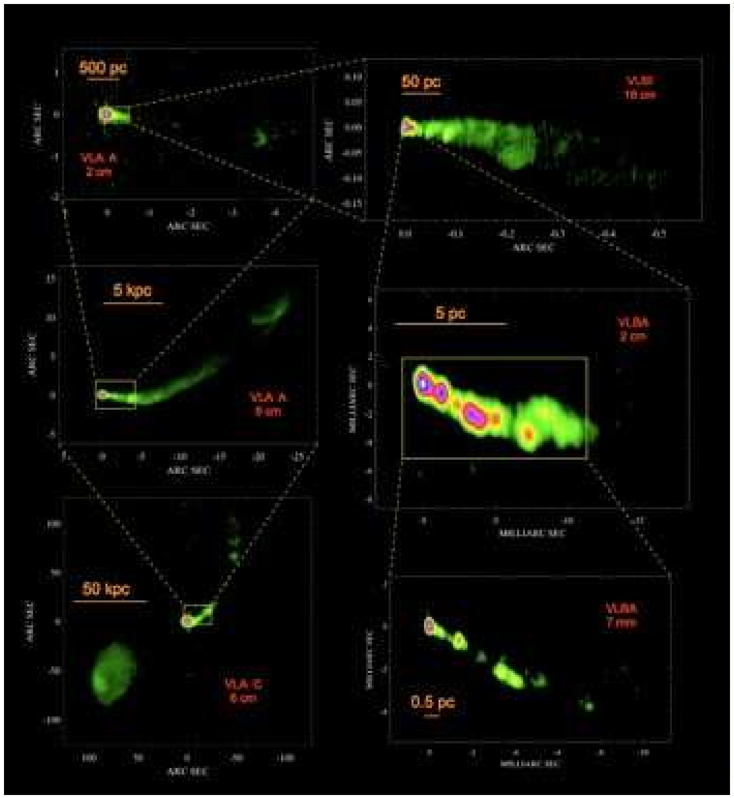

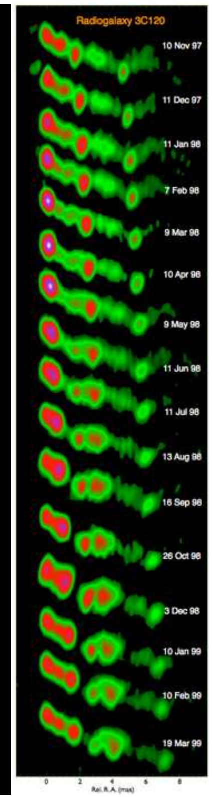

- better resolution with VLBI (Very Long Base Interferometry); shorter wavelengths
- corelator: interference of the coherent waves from VLBI sites

Synchrotron radiation from AGN jets: M87

Mechanisms of jet formation

- Blandford-Payne mechanism (1982): MHD flow – the jet can be launched and collimated by centrifugal and magnetic forces – the disk particles are driven upwards by the gradient of the pressure in the disk to fill the corona around the disk and are further accelerated by the gradient of the magnetic pressure

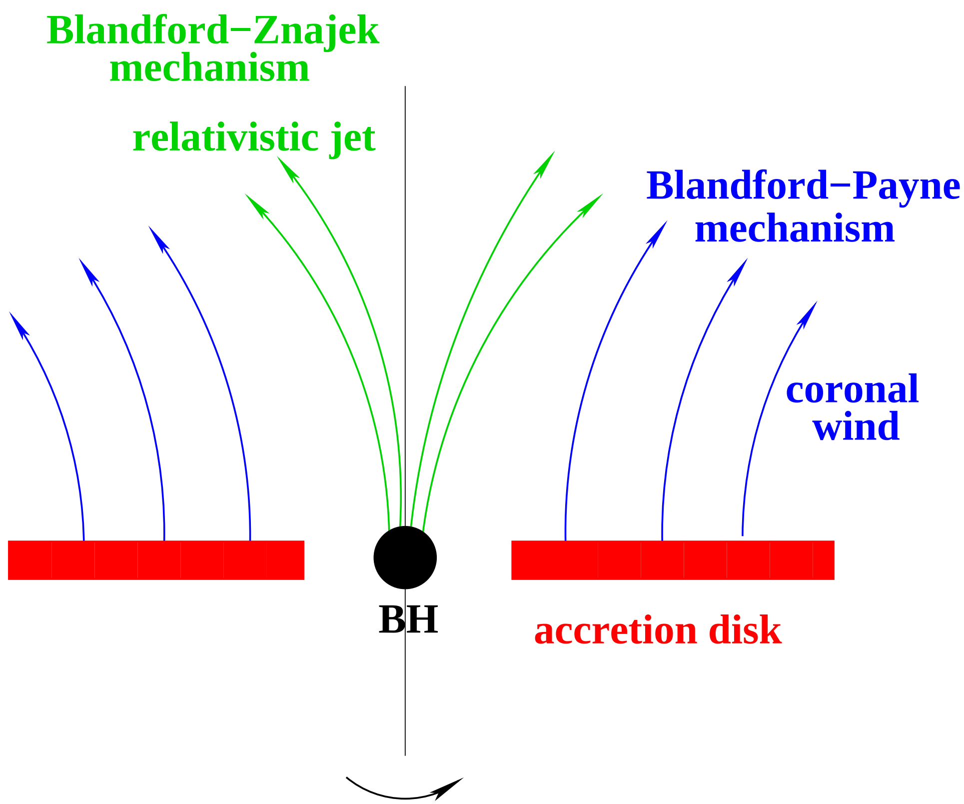

Mechanisms of jet formation

- Blandford-Znajek mechanism (1977): electromagnetically extraction of energy and angular momentum of a BH ("BH dynamo" mechanism) → the energy flux of the jets is provided by conversion of the BH rotational energy into Poynting flux, which is then dissipated at large distances from the BH by current instabilities

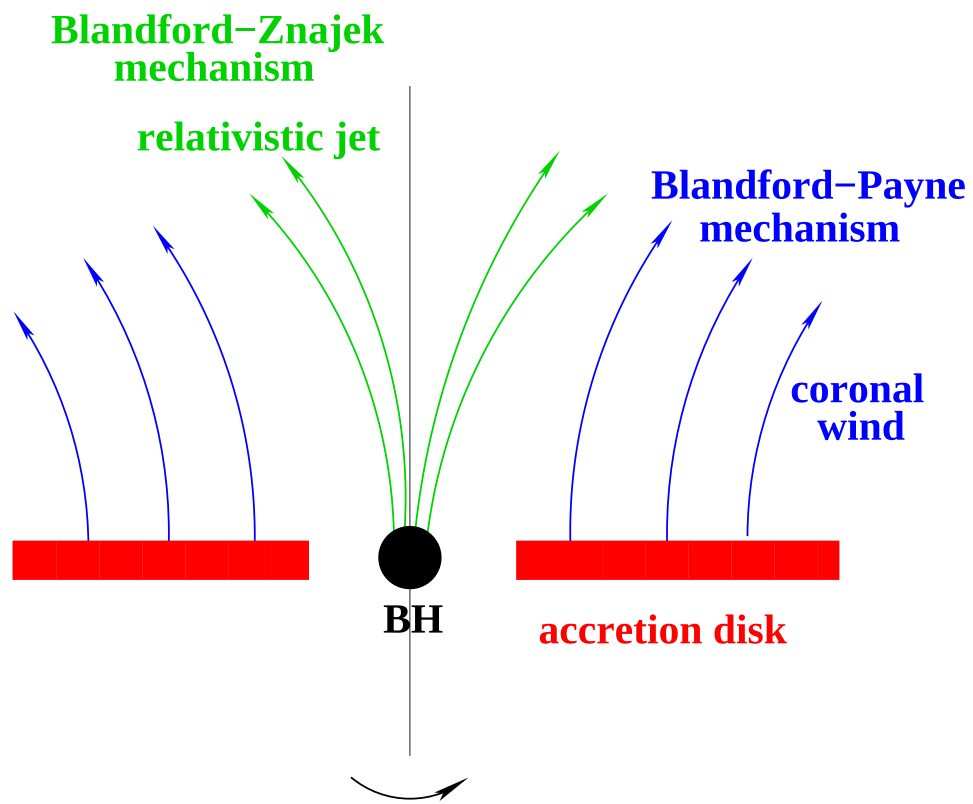

Structure of the jet

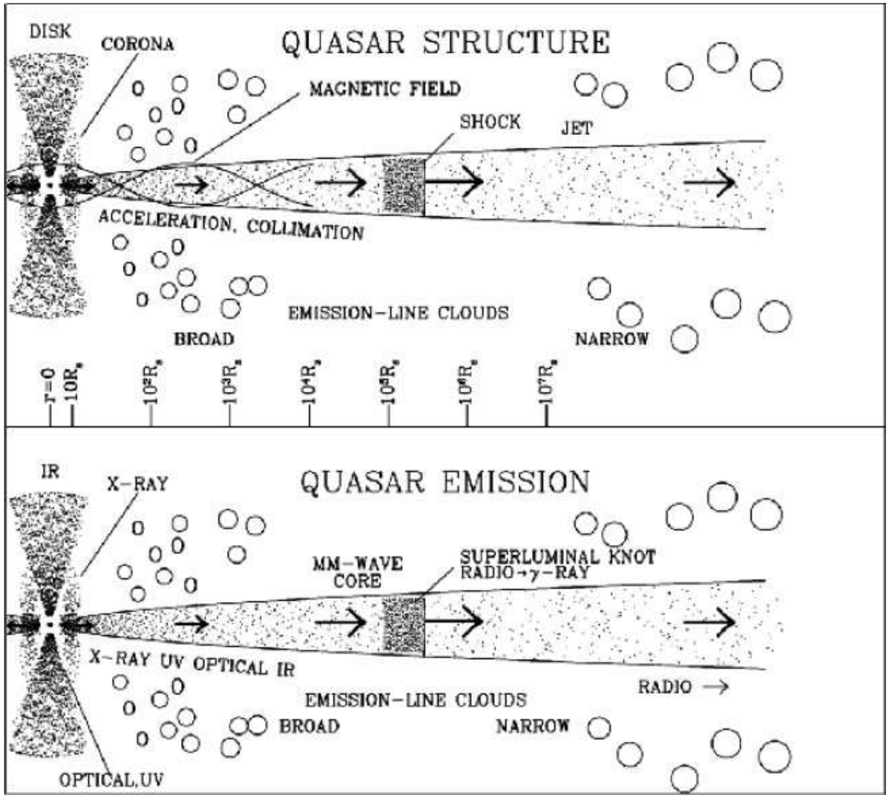

Marscher2000

- structure and emission of a radio-loud AGN
- helical magnetic fields
- synchrotron and inverse Compton radiation

Space plasmas

- plasmas may be collisional (e.g., fusion plasma) or collisionless (e.g., space plasma)

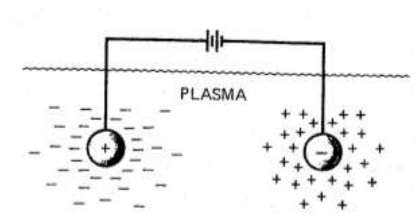

Debye shielding.

- Debye length (λ_D) = thickness of the cloud (sheath)
- L = length of a system; if $L \gg \lambda_D \rightarrow$ quasi-neutral plasma ($n_i \simeq n_i \simeq n$, plasma density)
- N_D = particles in a Debye sphere; if $N_D \gg 1 \rightarrow$ collective behavior
- τ_c = Coulomb collision time between e^-'s and ions; ω = frequency of a variation in the plasma; if $\tau_c \omega \gg 1 \rightarrow$ collisionless
- it is the characteristic frequency by which quasi-neutrality in a plasma can be violated if no external electric fields are applied

Space plasmas

Characteristic time and length scales

$$\omega_p = \left(\frac{4\pi ne^2}{m}\right)^{1/2}$$

Plasma frequency

$$\lambda_D = \frac{V_{thermal}}{\omega_p} \propto \left(\frac{T}{n}\right)^{1/2}$$

Debye length

$$\lambda_{skin} = c/\omega_p$$

skin depth

$$\omega_c = \frac{eB}{mc}$$

Larmor

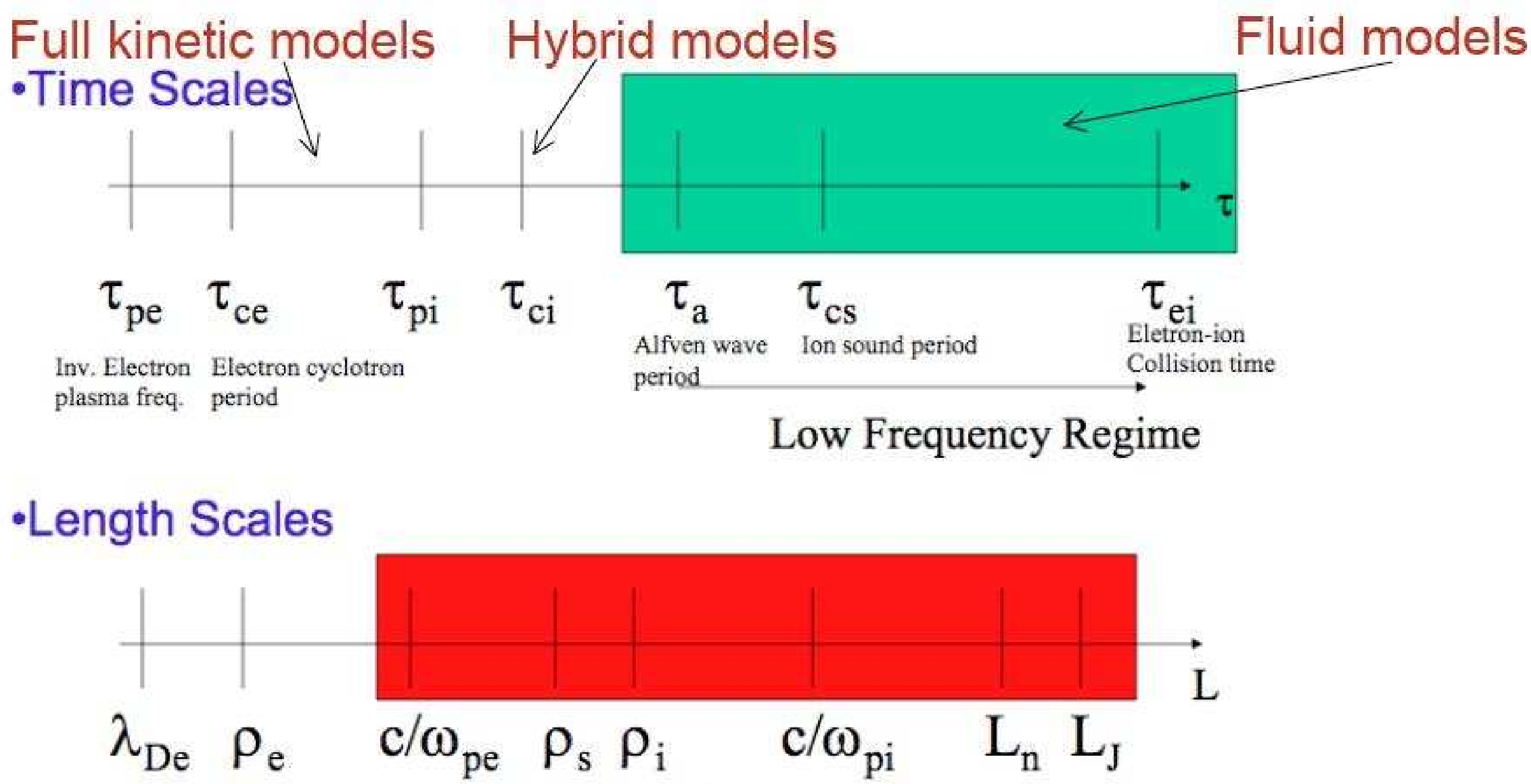

Space plasmas

- space plasmas differ by charge (e_j), mass (m_j), temperature (T_j), density (ρ_j), bulk speed (u_j), and thermal speed ($v_j = (k_B T_j/m_j)^{1/2}$) of the particles (of species j) by which they are composed
- they are mostly magnetized (internal and external magnetic fields)
- space plasmas are treated in several ways:
  - particle-in-cell (PIC) (microscopic – kinetic)
  - magnetohydrodynamics, MHD (macroscopic – fluid, high-density plasma)
  - hybrid (fluid electron and kinetic ions)
  - MHD with test particles (fluid mixed with particles)
  - particles with photons
- kinetic theory describes the plasma statistically, i.e. the collective behavior of the various particles under the influence of their self-generated electromagnetic fields; at low densities (particle collisions are negligible)

Space plasmas

- because of a multitude of free-energy sources in space plasmas, a very large number of instabilities can develop:
  - comparable to macroscopic size (e.g., bulk scale of plasma) $\rightarrow$ macroinstability (affects plasma globally)
  - comparable to microscopic scale (e.g., gyroradius) $\rightarrow$ microinstability (affects plasma locally)
- generation of instability is the general way of redistributing energy which was accumulated in a non-equilibrium state
- theoretical treatment:
  - macroinstability: fluid plasma theory (MHD)
  - microinstability: kinetic plasma theory (PIC)

Space plasmas

- a small perturbation in quantity A, which leads to a consistent perturbation in quantity B. An instability occurs if the perturbation in quantity B, in turn, enhances the initial perturbation in quantity A
- plasma instabilities for astrophysics are:
  - Weibel instability: driven by the thermal anisotropy (anisotropic distribution function); current filamentation
  - KH instability: driven by velocity shearing plasmas
- both instabilities manifest in currents that generate magnetic fields

Weibel instability

- PIC simulations of Weibel instability (Nishikawa et al. 2005+): Weibel instability creates filamented currents and densities along the jets
- Weibel instability mediates collisionless relativistic shocks (Medvedev 2009)
- (a) linear regime = current filamentation; (b) saturation; (c) nonlinear regime = filament coalescence

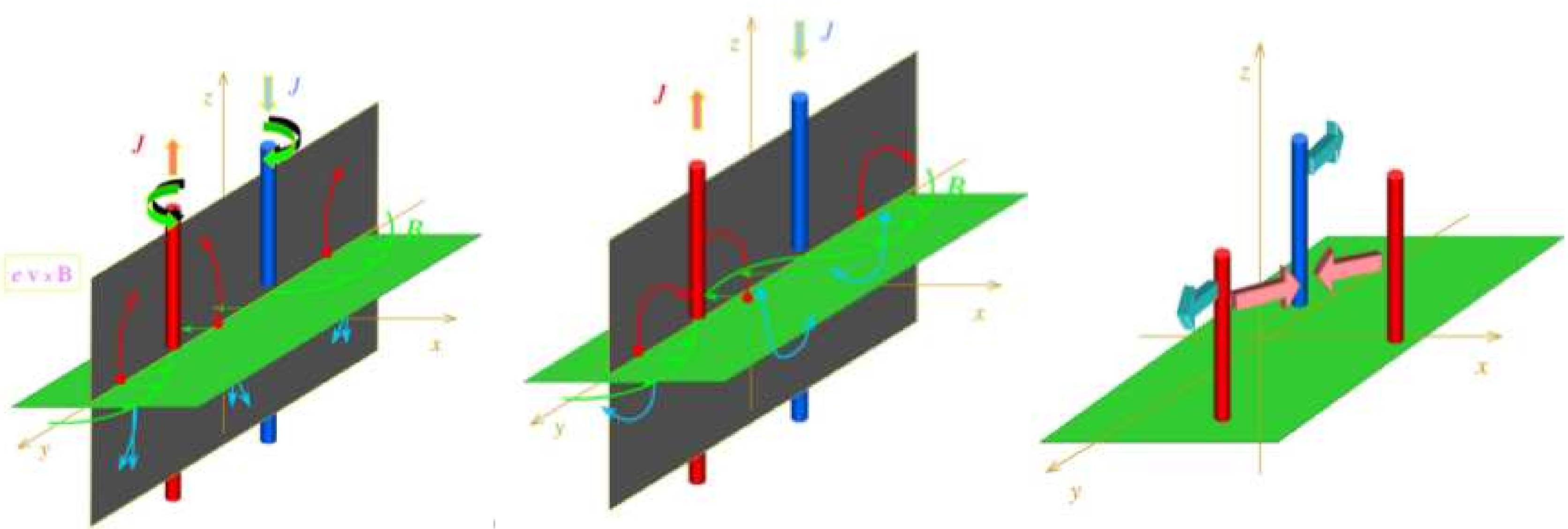

Weibel instability

3-D isosurfaces of z-component of current Jz for narrow jet (γv||=12.57)

electron-ion ambient t = 59.8ωe-1

-Jz (red), +Jz (blue), magnetic field lines (white)

Particle acceleration due to the local reconnections during merging current filaments at the nonlinear stage

thin filaments

merged filaments

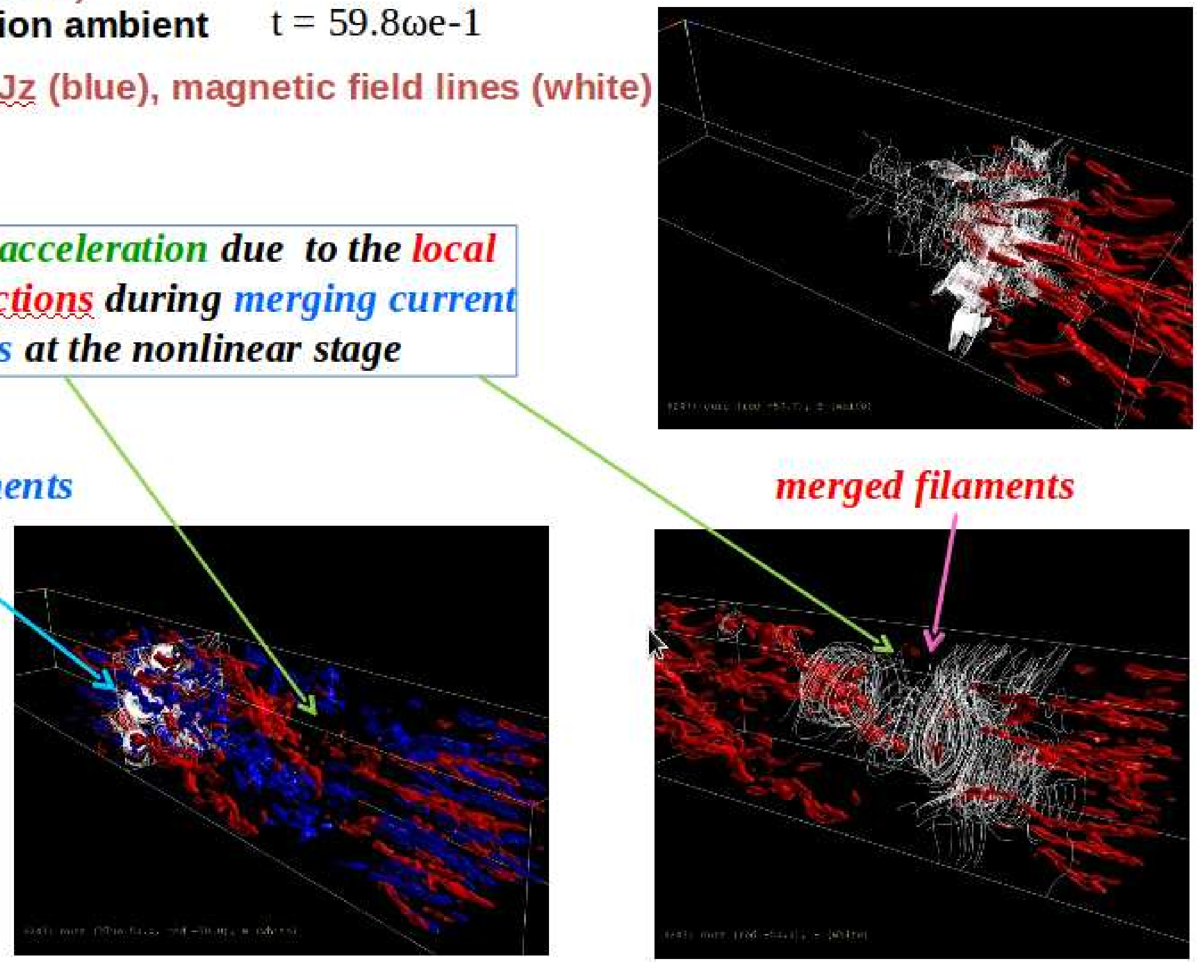

- Nishikawa et al. (2005+)

Kelvin-Helmholtz instability

- term Kelvin-Helmholtz was originally applied to a particular set of gravity-wave phenomena at discontinuities (Helmholtz 1868)
- its signature: vortices
- in real ocean and atmosphere
- in space strong velocity shears are present, triggering the collisionless KHI

- Jupiter (red spot), from the solar wind into planetary magnetospheres, in accretion disks, jets

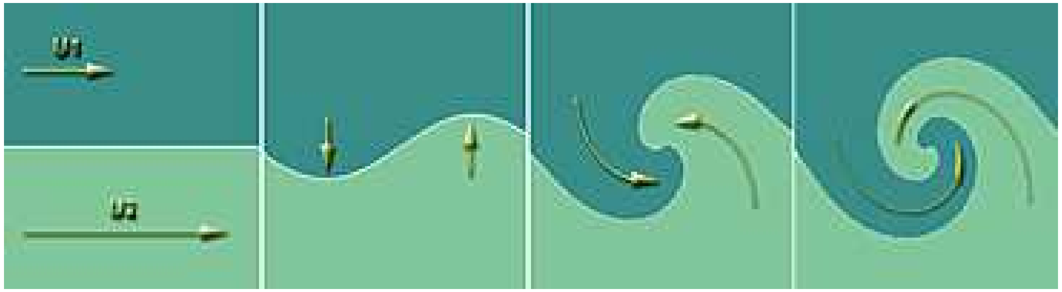

Kelvin-Helmholtz instability

- Alves et al. (2012): OSIRIS code (Fonseca et al. 2002)
- two counter streaming unmagnetized flows; equal densities; (non)relativistic flows; $e^- p^+$ and $e^- e^+$
- here: nonrelativistic flows, $e^- p^+$

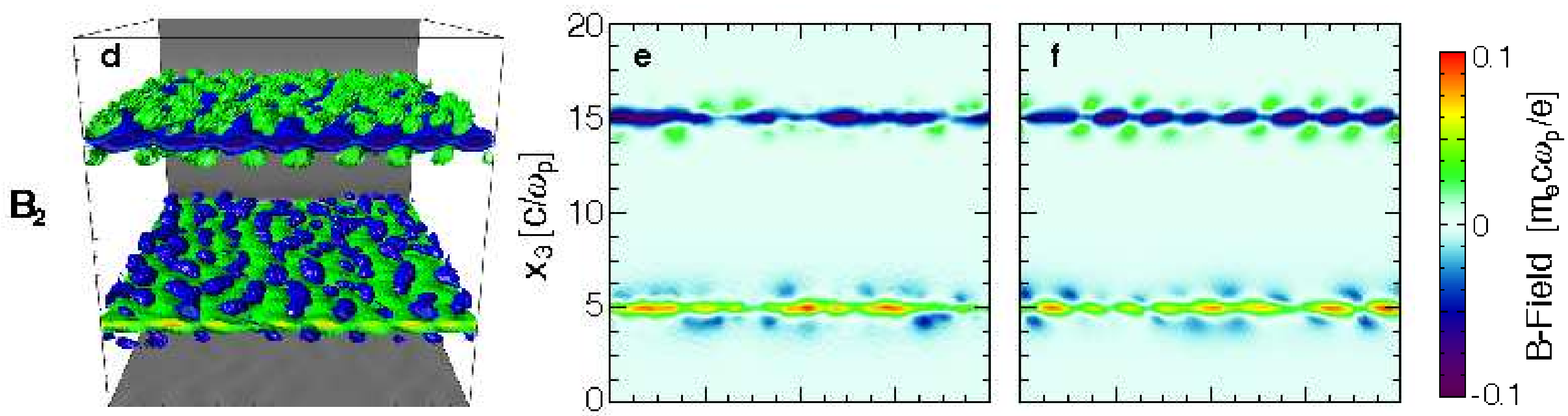

x_1 x_2 x_1

Simulation of kinetic Kelvin-Helmholz instability

work with Ken Nishikawa

Importance of studying KHI

- observations of the TeV BL Lac objects show brightenings and rapid variability in their TeV emission $\rightarrow$ high Lorentz factor flows occurring at smaller scale $\rightarrow$ ultra-relativistic bulk motion of the (inner) jet
- radio observations with VLBI of the pc-scale jet structure indicate a broad, slower (albeit relativistic) moving outflow
- a two-component jet structure: fast, low-density inner spine and slow, high-density sheaths
- instability of relativistic jet is important for understanding the observed jet structure & radiation

- TRIdimensional STANford (TRISTAN) code (Buneman, Nishikawa, & Neubert 1993)
- Modified by Ken Nishikawa for studying jets
- self-consistently solves the full set of Maxwell's equations, along with the relativistic equations of motion for the charged particles
- Maxwell's equations, Lorentz's force, Poisson's equation:

$$\frac{\partial \mathbf{E}_{\mathrm{T}}}{\partial t} = c^2 \nabla \times \mathbf{B}_{\mathrm{T}} - \mathbf{J}_{\mathrm{T}}, \quad \frac{\partial \mathbf{B}_{\mathrm{T}}}{\partial t} = -\nabla \times \mathbf{E}_{\mathrm{T}}$$

$$F_{\mathrm{L}} = 4\pi q_{\mathrm{T}} (\mathbf{E}_{\mathrm{T}} + \mathbf{v} \times \mathbf{B}_{\mathrm{T}}), \quad \nabla \cdot \mathbf{E}_{\mathrm{T}} = \rho$$

- discretize the Maxwell's and Lorentz's force equations on a grid with spacing Δx and timestep Δt
- Courant condition: $c\Delta t / \Delta x = C$, $C < 1$ (usually, $C < 0.5$ for stability)

R-PIC code

- fields are discretized on a finite 3D mesh (the computational grid); 3D Yee mesh is used to store the magnetic and electric fields

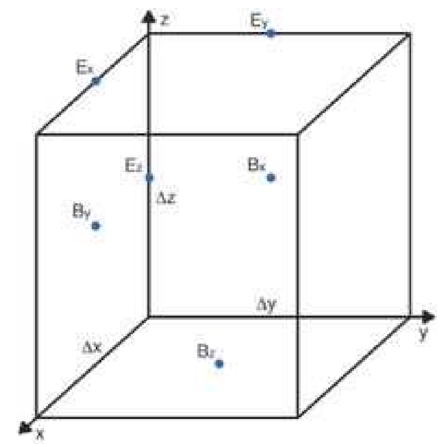

- a tri-linear interpolation function (linear in each spatial dimension) is used to interpolate the electric and magnetic fields to the particles positions

- PIC uses computational particles (called macro-particles) composed of ions and electrons

- weight factors for each node volume

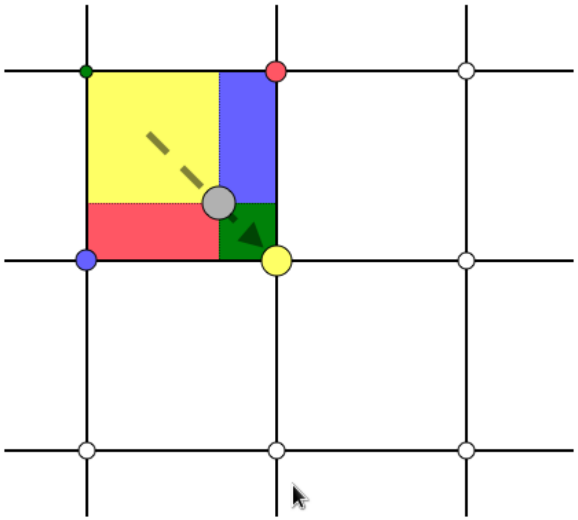

- fields are discretized on a finite 3D mesh (the computational grid); 3D Yee mesh is used to store the magnetic and electric fields

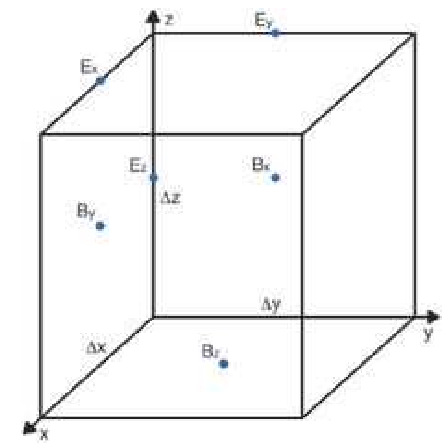

- a tri-linear interpolation function (linear in each spatial dimension) is used to interpolate the electric and magnetic fields to the particles positions
- these fields are then used to advance the velocity of the particles in time via the Lorentz force equation
- charges and currents derived from the particles velocities and positions are then used as source terms to re-calculate the electromagnetic fields

R-PIC code

$$\frac{v_i^{n+1/2} - v_i^{n-1/2}}{\Delta t} = \frac{F_i}{m_i}$$

$$\frac{x_i^{n+1} - x_i^n}{\Delta t} = v_i^{n+1/2}$$

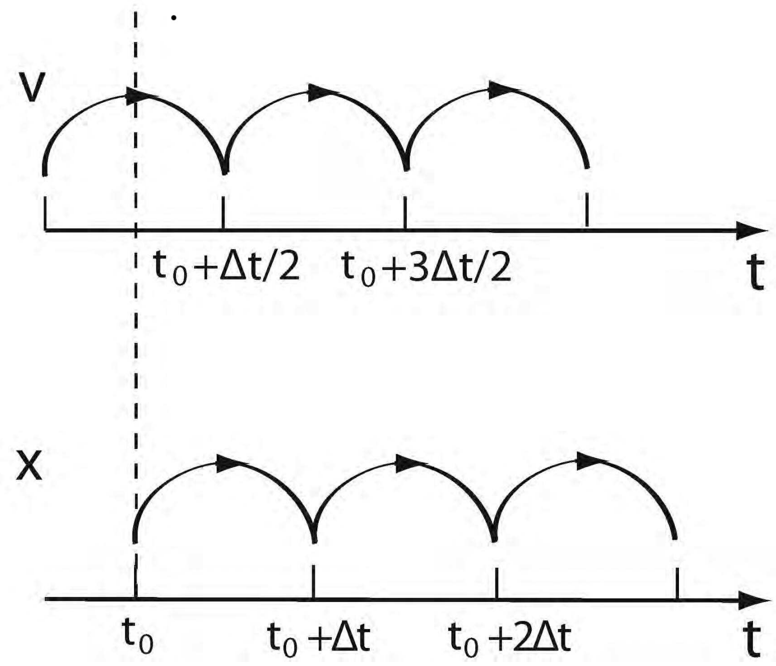

R-PIC code

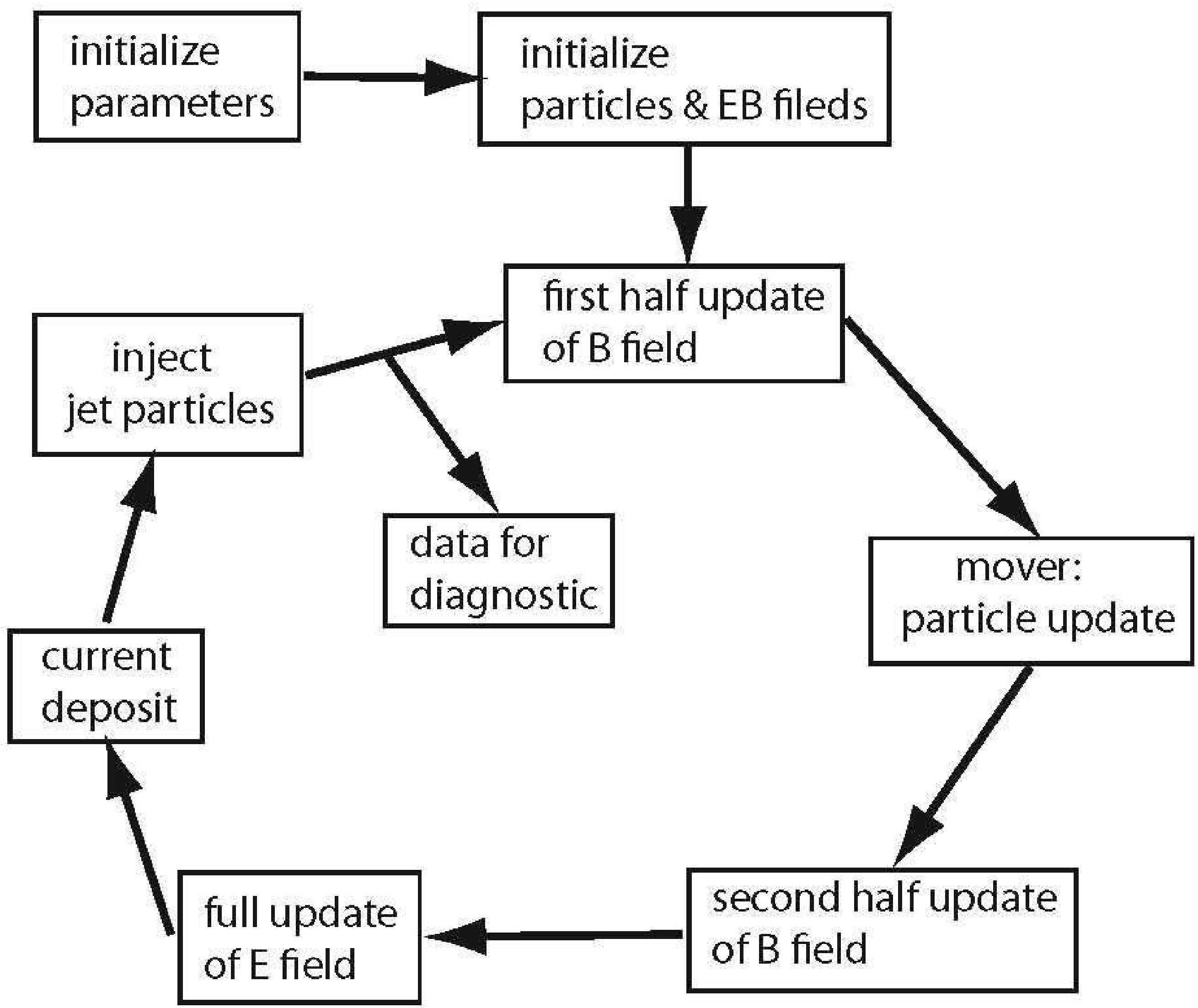

initialize parameters
initialize particles & EB fileds
first half update of B field
mover: particle update
second half update of B field
full update of E field
current deposit
inject jet particles
data for diagnostic

Initial conditions and numerical results

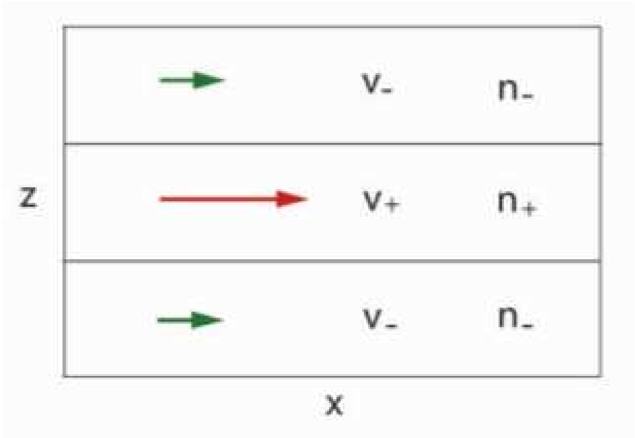

- a stationary plasma in the upper and lower quarters of the simulation box and a relativistic core jet with $\gamma = 15$ in the middle-half of the box; unmagnetized
- size of the box: $1005 \times 205 \times 205\Delta^3$
- 8 particles/cell
- mass ratio of ion and electron, $m_\mathrm{i}/m_\mathrm{e} = 20$
- periodic boundary conditions in all directions

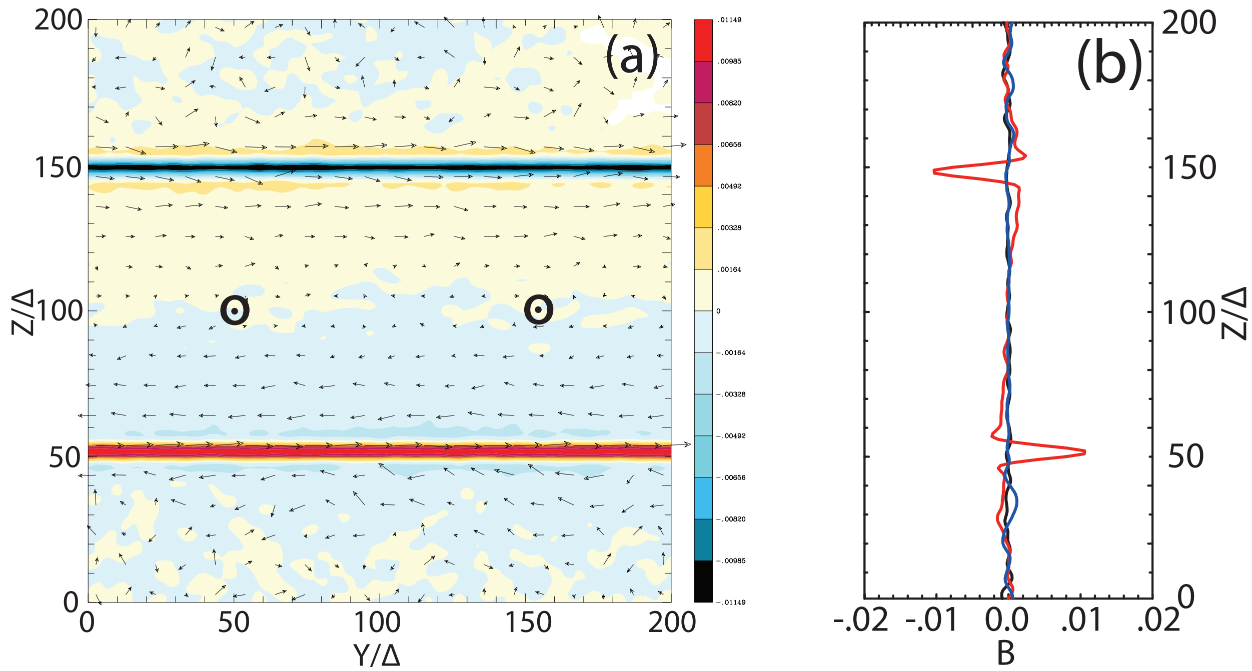

- magnetic field structures generated by shearing relativistic electron-ion flows taken at time $t = 70\,\omega_{pe}^{-1}$; B_y is plotted in the $y - z$ plane at the center of the box $x = 500\Delta$

- (a) jet out of the plane, in the $x - z$ plane at the center of the box $y = 100\Delta$

- (b) B_x (black), B_y (red), and B_z (blue) at $x = 500\Delta$ and $y = 100\Delta$

R-PIC code

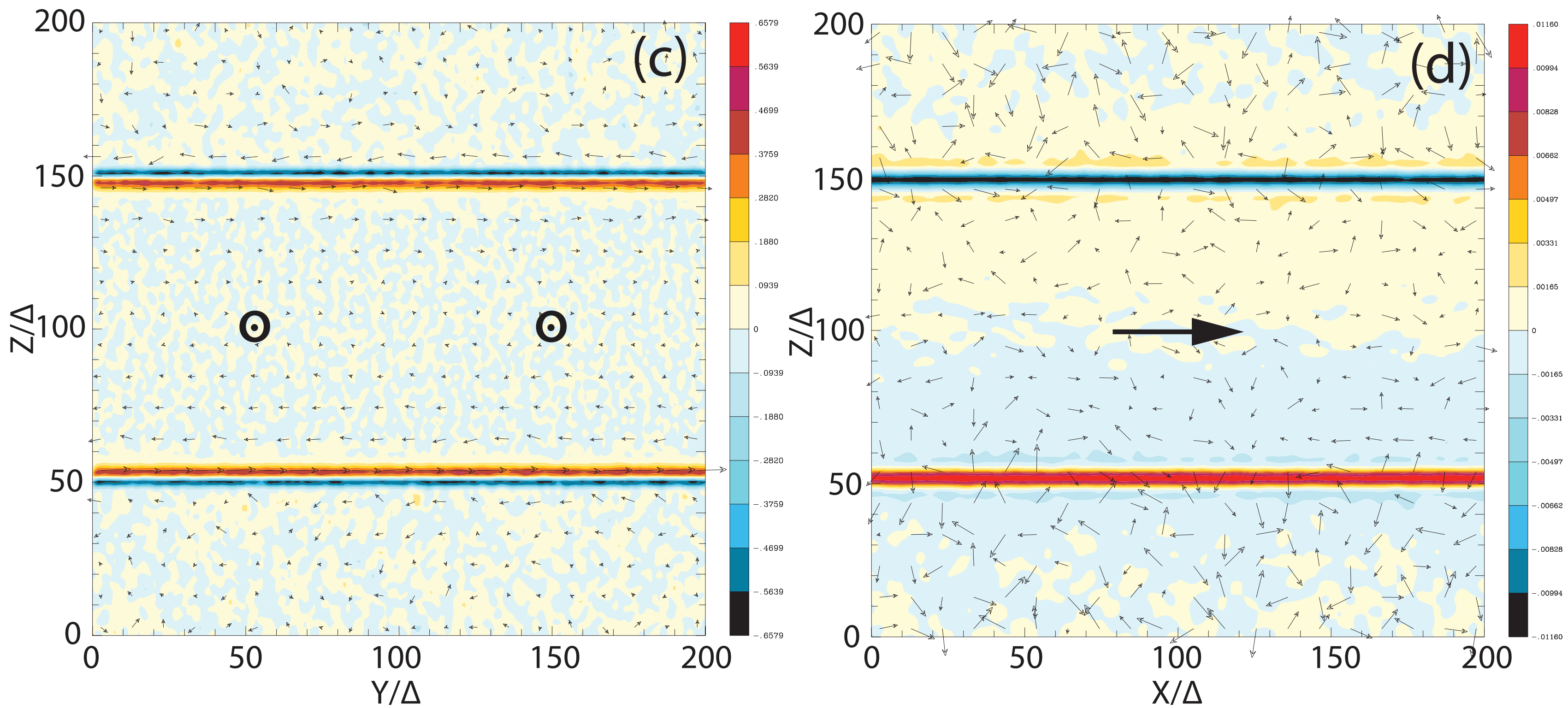

- (c) shows the *x* component of current; the relativistic jet is out of the plane and the positive current is generated at the core jet side and the negative current is generated in the sheath side
- (d) same as (a) but it shows one fifth of the simulation size to show the details

Summary and conclusions

Summary and conclusions

- we use the R-PIC code developed by Nishikawa et al. (2005+) to simulate the generation of magnetic fields at the separation layer between two plasma sheaths by the Kelvin-Helmholtz instability
- such generation of the magnetic fields is relevant for synchrotron models that operate in astrophysical jets
- further work: calculate the radiation emitted by charged particles in interaction with such magnetic fields, including the time evolution of a spectrum, and compare with observational data
- compare the numerical results with those obtained by Alves et al. (2012)